

Multi-qubit time-bin quantum RAM

E. S. Moiseev

*Institute for Quantum Science and Technology, University of Calgary, Canada and
Kazan (Volga Region) Federal University, Russia*

S. A. Moiseev*

Kazan Quantum Center, Kazan National Research Technical University, Kazan, Russia

We have proposed a scheme of multi-qubit *quantum random access memory* (qRAM) based on the impedance matched photon echo quantum memory incorporated together with the control three-level atom in two coupled QED cavities. A set of matching conditions for basic physical parameters of the qRAM scheme that provides an efficient quantum control of the fast single photon storage and read-out has been found. In particular, it was found that the qRAM operation is determined by the properties of the photonic molecular realized in the qRAM dynamics. Herein, the maximal efficiency of the qRAM is achieved when the cooperativity parameter of the photonic molecular equals to unity that can be easily experimentally implemented. The quantum address of the stored photonic qubits can be put into practice when the address is encoded in photonic multi-time-bin state. We discuss the advantages of the qRAM in terms of working with multi-qubit states and the implementation by current quantum technologies in the optical and microwave domains.

PACS numbers: 03.67.Hk, 03.67.Lx, 42.50.Md, 42.50.Ex

Keywords: quantum information, optical quantum memory, cavity QED, quantum random access memory, photon time-bin qubit, photonic molecular.

INTRODUCTION

The elaboration of the universal quantum computing and quantum communication requires qRAM for the implementation of basic protocols such as a quantum search over the classical database, discrete logarithms, quantum Fourier transformation, collision finding and quantum digital signature [1–4]. The qRAM was proposed by Giovanetti et al. [5] and developed [6] in the bucket-brigade architecture. The qRAM provides the arbitrary access to the data cells ($|D_n\rangle_d$) by the quantum superposition of the address states ($|\Psi^a\rangle = \sum_n \alpha_n |\psi_n^a\rangle$): $|\Psi^a\rangle \xrightarrow{\text{qRAM}} \sum_{n=1}^N \alpha_n |\psi_n^a\rangle |D_n\rangle_d$ [5]. Exponential speed-up over the classical computation requires an operation of qRAM with large number of qubits. Such qRAM should be also compact and integrable in the quantum network [7] and in the developing hybrid quantum circuits [8]. We propose using the photon echo based *quantum memory* (QM) technique [9, 10] for the implementation of such qRAM. This choice seems reasonable due to a number of promising experimental results obtained in this QM technique for the effective storage of single photon fields. Herein, the photon echo QM technique has demonstrated the record efficiency [11, 12], and the optical multimode quantum storage [13, 14] of up to 1000 temporal light modes [15]. More recently the photon echo QM was developed [16] and demonstrated [17] for the atomic ensembles in the impedance matching QED cavity that opens a practical way for implementing compact multi-qubit QM devices. Such photon echo QM is also applicable for the microwave spectral range [18], for the integration in quantum computer schemes [19] and it can work

efficiently with intensive quantum light fields [20].

In this work we propose the architecture of multi-qubit qRAM consisting of the photon echo QM unit containing N resonant atoms and control three-level atom situated in two coupled QED cavities. We found the optimal physical parameters of the qRAM providing the maximal performance and proposed a scheme for addressing storage of the photon qubit. We also discussed potential implementations of the proposed qRAM in the optical and microwave domains on the basis of current technologies.

PRINCIPAL SCHEME

The diagram of the proposed qRAM is shown in Fig. 1. The scheme operation is controlled by the three-level atom. The control atom is strongly coupled to the QED cavity mode that is used for the implementation of the transistor effect for the quantum transport of the input photon to the QM atomic ensemble (there are a number of different physical implementations for a three-level quantum system in the resonant cavity which could be discussed by taking into account certain physical parameters of the analyzed qRAM). If the control atom is in the ground state, it will reflect the incoming photon back, however, if the atom is far off the resonance, the incoming photon will be ideally recorded into the QM unit. We show how the controlled photon transport can be made reversible and efficient for the implementation of qRAM.

By assuming that the control atom is in the ground state $|g_c\rangle$, the interaction of the input photon with resonant QED cavities and all atoms is described by the wave function:

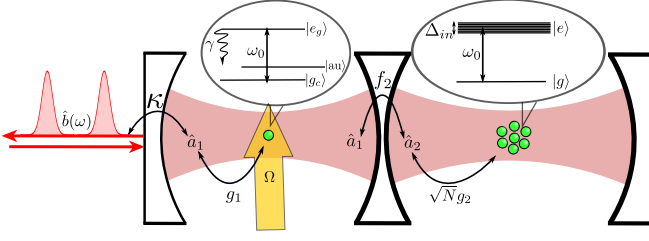


FIG. 1. (Color online) Free propagating modes $\hat{b}(\omega)$ are coupled to the double sided QED cavity with the mode \hat{a}_1 . This cavity contains a single three-level atom with the quantum transition ($|g_c\rangle \leftrightarrow |e_c\rangle$) resonant to the cavity mode \hat{a}_1 characterized by the frequency ω_0 , coupling constant g_1 , and decay rate γ due to the interaction with transverse field modes $\hat{c}_m(\nu)$; κ is the decay rate of the cavity mode into the free propagating modes $\hat{b}(\omega)$, arrow with Ω means the control laser field with the Rabi frequency on the transition $|g_c\rangle \leftrightarrow |a_u\rangle$. The other side of the cavity is coupled (with the rate f_2) to the second cavity with a two-level atomic ensemble. The atoms have the inhomogeneous broadening Δ_{in} of the resonant line and the collective coupling constant $\sqrt{N}g_2$ for the interaction with the cavity mode.

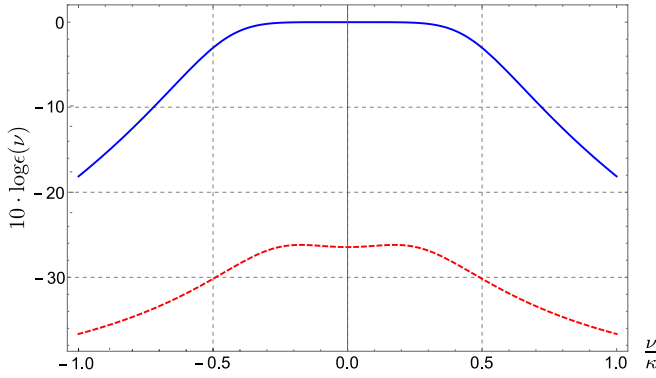


FIG. 2. (Color online) Spectral transfer function in the logarithmic scale $10 \log \epsilon(\nu/\kappa)$ for the single photon storage (blue solid line) and for the blockade (red dashed line). The wide spectral window for the photonic storage is implementing by three impedance matching conditions: $C_{QT} = 1$ and Eqs. (7),(8). The strong blockade of the memory process is represented for the single atom cooperativity factor $C = 10$ and $\gamma = \kappa$.

$$|\Psi(t)\rangle = \left(\beta_c \hat{S}_+^0 + \sum_{j=1}^N \beta_j \hat{S}_+^j + \alpha_1 \hat{a}_1^\dagger + \alpha_2 \hat{a}_2^\dagger + \int d\nu \alpha_\nu \hat{b}^\dagger(\nu) + \sum_m \int d\omega r_\nu^m \hat{c}_m^\dagger(\nu) \right) |0\rangle_f |g_c\rangle |g\rangle, (1)$$

with the normalization $|\beta_c|^2 + \sum_{j=1}^N |\beta_j|^2 + |\alpha_1|^2 + |\alpha_2|^2 + \int d\nu |\alpha_\nu|^2 + \sum_m \int d\nu |r_\nu^m|^2 = 1$ and the initial quantum state: $|\Psi(t \rightarrow -\infty)\rangle = |\psi_{in}(t)\rangle_f =$

$\int d\nu \alpha_\nu^0(t) \hat{b}_\dagger(\nu) |0\rangle_f$; $\alpha_\nu^0 = \alpha_\nu(-\infty)$ characterizes the state of the input photon wave packet; $\int d\nu |\alpha_\nu^0|^2 = 1$; $\beta_c = \beta_j = \alpha_{1,2} = r_\nu^m = 0$; $|0\rangle_f$ is the vacuum state of the input light modes; $|g_c\rangle$ and $|g\rangle \equiv \prod_{j=1}^N |g_j\rangle$ are the ground states of the control atom-c and QM atoms, where \hat{S}_z^0 , \hat{S}_z^j are z-projections of the effective spin 1/2 operators on the $|g_{c,j}\rangle \rightarrow |e_{c,j}\rangle$ transition, \hat{S}_+^j , \hat{S}_-^j and \hat{S}_+^0 , \hat{S}_-^0 are the transition spin operators of j -th and control atoms; $\hat{a}_{1,2}^\dagger$ and $\hat{a}_{1,2}$ are arising and decreasing operators of the 1-st and 2-nd cavity field modes; $\hat{b}^\dagger(\nu)$, $\hat{b}(\nu)$ are the bosonic operators of free propagating modes ($[\hat{b}(\nu), \hat{b}^\dagger(\nu')] = \delta(\nu - \nu')$); $\hat{c}_m(\nu)$, $\hat{c}_m^\dagger(\nu)$ are the bosonic operators of the bath interacting with the control atom in the first cavity ($[\hat{c}_m(\nu), \hat{c}_n^\dagger(\nu')] = \delta_{m,n} \delta(\nu - \nu')$).

By using the well-known input-output formalism [21], we solve the Schrödinger equation for the wave function $|\Psi(t)\rangle$ that gives the following amplitudes for the large time of the interaction $t > \delta t$ (where δt is the temporal duration of the input photon wavepacket):

$$\beta_j(\Delta_j, t) = i\sqrt{2\pi\kappa} \frac{g_2}{f_2} F(\Delta_j) \alpha_{\Delta_j}^0 e^{-i(\Delta_j - i/T_2)t}, \quad (2)$$

$$F(\Delta) = \frac{f_2^2}{(Ng_2^2 \tilde{G}(\Delta) - i\Delta)(\frac{\kappa}{2} + \frac{ig_1^2}{\Delta - \delta + \frac{i}{2}\gamma} - i\Delta) + f_2^2}, \quad (3)$$

where $\tilde{G}(\Delta) = \int d\nu \frac{G(\nu)}{\epsilon + i(\nu - \Delta)}$, $G(\nu)$ is the formfactor of the *inhomogeneously broadened* (IB) resonant line; we also used the continuous limit for the large number of atoms in QM: $\beta_j(\Delta_j, \tau) \rightarrow \beta(\Delta, \tau)$, $\sum_{j=1}^N \dots \rightarrow N \int d\Delta G(\Delta) \dots$, T_2 is the decoherence time of the atomic ensemble in QM.

We find the probability of the photon transfer in QM using $\beta(\Delta, \tau)$: $P_a(t > \delta t) = \sum_{j=1}^N |\beta_j(t)|^2 = \int_{-\infty}^{\infty} d\Delta \epsilon(\Delta) |\alpha_\Delta^0|^2$. Analogous to any classical spectral device, qRAM can be characterized by its spectral efficiency $\epsilon(\Delta) = 2\pi N \kappa |\frac{g_2}{f_2}|^2 |G(\Delta)|^2 |F(\Delta)|^2$ for the single photon storage. For simplicity but without loss of generalization, we assume IB to be Lorentzian $G(\nu) \equiv G_L(\nu) = \frac{\Delta_{in}}{\pi(\nu^2 + \Delta_{in}^2)}$ with the bandwidth Δ_{in} . For the narrow bandwidth of the input photon field ($\delta\omega_f \sim \delta t^{-1} \ll \kappa, \Delta_{in}$), we find the following spectral efficiency

$$\epsilon(\Delta \approx 0) = \frac{4C_{pm}}{(1 + C_{pm} + \frac{\gamma^2 C}{\delta^2 + (\gamma/2)^2})^2 + (\frac{2\delta\gamma C}{\delta^2 + (\gamma/2)^2})^2}, \quad (4)$$

determining the main properties of qRAM, where $C = \frac{g_1^2}{\kappa\gamma}$ is a well-known single atom cooperativity factor; we also introduced the *cooperativity factor of photonic molecular* for the analyzed qRAM: $C_{pm} = |f_2|^2 / (\kappa \frac{Ng_2^2}{2\Delta_{in}})$. The

factor C_{pm} reflects the quantum and dissipative properties of the photon in two coupled QED cavities, since f_2 is the interaction constant between the two quantum states of the photon, i.e. the coupling constant between the two states of the photonic molecular (the photon exists in the first or in the second QED cavity), while κ and $Ng_2^2/(2\Delta_{in})$ are the decay constants of the photon states in these QED cavities.

By analyzing Eq. (4), we find two basic regimes of the qRAM operation: 1) Storage of a single photon in the QM ensemble and 2) Blockade of the photon storage (retrieval) in (from) the QM ensemble.

1) Perfect storage is implemented for the large spectral detuning of the control atom $|\delta| \gg \gamma C$. It can be implemented by transferring the atom in the third ancillary state $|au_c\rangle$ (see Fig.1) (4) where the resonant storage efficiency is:

$$\epsilon(0) |_{|\delta| \gg \gamma C} \equiv \epsilon_T(0) = 4C_{pm}/(1 + C_{pm})^2, \quad (5)$$

that shows the ideal transmission (index "T" in ϵ) of single photon in the QM ensemble (5) at $C_{pm} = 1$, which is the first *impedance matching* (IM) condition of the effective qRAM. Equation (5) with $\epsilon(0) = 1$ at $C_{pm} = 1$ reproduces properties, which are similar to the properties of the impedance matching photon echo QM [16] but in the presence of the additional strongly interacting QED cavity mode. Herein, the impedance photon echo QM [16] is characterized by the different coupling constant $2N|g_2|^2$ and the following two decay constants κ , Δ_{in} . These parameters satisfy the impedance matching condition $\kappa\Delta_{in} = 2N|g_2|^2$ (it is possible to generalize this condition and facilitate its implementation by transferring to the off-resonant Raman echo QM scheme [22]). The impedance matching condition of qRAM couples somewhat different physical parameters and we will see how this new matching condition provides the convenient implementation of qRAM operations.

Analyzing $\epsilon(\nu)$ for the transfer process we found the second

$$\frac{N|g_2|^2}{\Delta_{in}} = \frac{\Delta_{in}\kappa/2}{(\Delta_{in} + \kappa/2)}, \quad (6)$$

and third

$$\Delta_{in} = \kappa/2, \quad (7)$$

IM conditions, where the spectral quantum efficiency $\epsilon(\nu)$ has the almost ideal flat spectral behavior (see Fig 2) around $\nu \approx 0$ that is given by the expression

$$\epsilon_T(\nu) = \frac{1}{1 + (\frac{\nu}{\kappa/2})^6}, \quad (8)$$

and providing the efficient transfer of the broadband input single photon field. This process transfers the wave function (1) into the purely atomic state $|\Psi(t > \delta t)\rangle \cong |0\rangle_f |au\rangle_c \left(\sum_{j=1}^N \beta_j(t) \hat{S}_+^j \right) |g\rangle$.

2). In the case of the resonant interaction with the control atom (when the atom stays in the state $|g\rangle_c$ where $\delta = 0$) we find

$$\epsilon(0)_{|\delta=0} \equiv \epsilon_B(0) = 4C_{pm}/(1 + C_{pm} + 4C)^2, \quad (9)$$

that leads to

$$\epsilon_B(0)_{|C_{pm}=1} = (1 + 2C)^{-2}. \quad (10)$$

By using the single atom cooperativity factor C from the experimental data [8] for the single atom in the Fabry-Perot cavity $C \equiv C_{opt} = 30$ and for the superconducting qubit in the moderate microwave resonator $C \equiv C_{\mu w} = 300$, we get quite good blockade with $\epsilon_{B,opt} = 2.6 \cdot 10^{-4}$ and $\epsilon_{B,\mu w} \approx 3 \cdot 10^{-6}$. It is important to note that the choice of the most acceptable three-level quantum systems and the type of the QED cavities is still an open question for the further studies, where using photonic waveguides, nano-fibers and surface plasmon polaritons could be also promising for the experimental implementation.

The most important benchmark of the photon blockade is the reflection of the input photon field. The direct usage of the input-output relationship $\alpha_{in}(\nu) + \alpha_{out}(\nu) = \sqrt{\kappa}\alpha_1(\nu)$ and the relation $\alpha_1(\nu) = A_{1,in}(\nu)\alpha_{in}(\nu)$ (see $A_{1,in}(\nu)$ in the supplement material) leads to

$$\alpha_{out}(\nu) = f_{Bl}(\nu)\alpha_{in}(\nu), \quad (11)$$

where

$$f_{Bl}(\nu) = \frac{i\kappa}{\nu + \frac{i\kappa}{2} - \frac{g_1^2}{\nu - \delta + i\gamma/2} - \frac{f_2^2}{\nu + iN\tilde{g}_2^2\tilde{G}(\nu)}} - 1. \quad (12)$$

Here for sufficiently narrow spectral width of the storage light and resonant interaction with control atoms ($\delta = 0$) we obtain

$$f_{Bl}(|\nu| < \kappa) |_{\delta=0} \rightarrow \left(\frac{1}{\frac{1+C_{pm}}{2} + 2C} - 1 \right). \quad (13)$$

Taking into account here the first matching condition $C_{pm} = 1$ we find for Eq.(11)

$$\alpha_{out} = -\frac{2C}{(1 + 2C)}\alpha_{in}. \quad (14)$$

The reflection (14) is valid with high accuracy within the spectral width which is comparable with the memory storage window $\sim \kappa$ if all three IM conditions hold.

Inserting the same values for the single atom cooperativity factor we obtain $|\frac{\alpha_{out}}{\alpha_{in}}|^2 = 0.983$ and 0.996 for $C \equiv C_{opt} = 30$ and $C \equiv C_{\mu w} = 300$, respectively, i.e. the rather strong blockade (see Fig. 2).

By implementing the CRIB procedure for the retrieval of the stored single photon field, we invert the atomic detuning $\Delta_j \rightarrow -\Delta_j$ at the time $t = \tau$ (in general, one can also use some other experimental methods for rephasing the atomic coherence, such as AFC- or silent echo protocols, but CRIB is easier to be demonstrated due to its perfect time reversibility). Initially all free propagation modes and two cavity modes are in the vacuum state and the control atom is in the ground state, while the QM atomic coherence is given by $\beta_j(\Delta_j, \tau)$. Calculating the echo field emission (see the readout stage in the supplement materials), which occurs in the time reversal manner, we find the wave function of the light-atomic system for the time $t \gg 2\tau$ with the following spectral photonic amplitude $\alpha_\nu(t)$ is:

$$\alpha_\nu(t) = -2\pi\kappa N \left| \frac{g_2}{f_2} \right|^2 G_L(\nu) F_S(-\nu) F_R(\nu) \alpha_{-\nu}^0 e^{-i\nu(t-2\tau)-2\tau/T_2}, \quad (15)$$

where indices S, R denote the *storage* and the *retrieval* stages. Herein, if the control atom stays in the state $|au\rangle_c$ (i.e., $S, R \rightarrow T$), we find from Eq.(15) the following quantum efficiency of the stored photon retrieval:

$$P_{echo|\delta\omega_f \leq 0.2\kappa} \cong \frac{16C_{pm}^2 e^{-4\tau/T_2}}{(1+C_{pm})^4} |_{C_{pm}=1} = e^{-4\tau/T_2}, \quad (16)$$

where the wave function of the irradiated photon field is $\alpha_\nu(t) \cong -\alpha_{-\nu}^0 \exp\{-i\nu(t-2\tau)-2\tau/T_2\}$, that means the perfect time-reversal retrieval of the initial single photon state under the condition of the long-lived coherence time $2\tau/T_2 \ll 1$. The probability of the echo pulse retrieval for different decoherent time T_2 and pulse duration δt is presented in Fig. 3, where one can find the necessary relation between T_2 and other parameters.

For the case, when the control atom is prepared in the ground state $|g_c\rangle$, where $\delta = 0$, we implement the blockade for the photon retrieval (where the index $R \rightarrow B$). Here, under the condition of the perfect storage ($S \rightarrow T$) we obtain for the photon emission probability:

$$P_{echo} = e^{-4\tau/T_2} \int_{-\infty}^{\infty} d\Delta \epsilon_T(\Delta) \epsilon_B(\Delta) |\alpha_\Delta^0|^2 |_{\delta\omega_f \leq 0.2\kappa, C_{pf}=1} \cong \frac{e^{-4\tau/T_2}}{(1+2C)^2} |_{C \geq 10} < 0.0023, \quad (17)$$

that means the strong blockade of the stored state, when the echo photon is efficiently reabsorbed by the QM

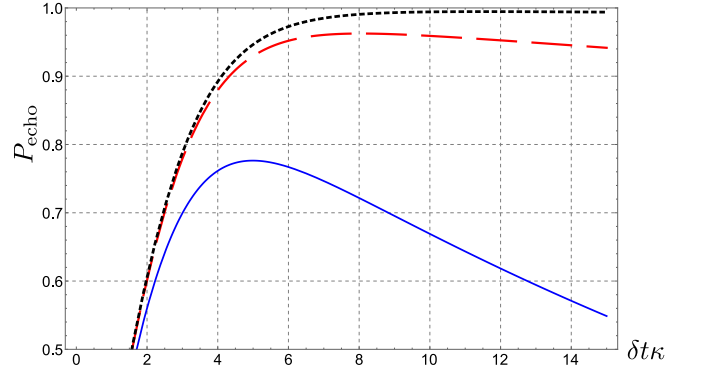


FIG. 3. (Color online). Probability of the echo pulse retrieval as a function of the Gaussian pulse duration δt (in units $\delta t \kappa$) for different atomic relaxation times T_2 : $T_2 \kappa = 10^2$ (blue, solid line); $T_2 \kappa = 10^3$ (red, long dashed line); $T_2 \kappa = 10^4$ (black, short dashed line) when three IM conditions hold.

atomic ensemble. The atomic amplitudes grasp the additional π -shift : $\beta(\Delta, \tau) e_i^{i\Delta t} \rightarrow -\beta(\Delta, \tau) e^{i\Delta t} e_{t > 2\tau}^{-(t-\tau)/T_2}$ as a result of the echo photon reabsorption. One can obtain Eqs. (15),(17) in the limit $1/T_2 \rightarrow 0$ by using the general approach based on the time reverse symmetry of light-atoms equations describing the qRAM operation for the retrieval stage.

QUANTUM ADDRESSING

Here we demonstrate the quantum addressing for the retrieval stage of the qRAM operation by assuming the rather large time T_2 of the atomic coherence ($T_2 \kappa \geq 10^4$, see Fig.3). Let us assume that M photon qubits prepared in the state $\prod_{n=1}^M |\psi_{in,m}(t-t_m)\rangle_f$ have been stored one by one in the atomic ensemble. Here, the qRAM is excited in the state

$$|Q_{RAM}\rangle = \hat{S}_{(M)}^+(t-t_M) \dots \hat{S}_{(1)}^+(t-t_1) |g\rangle_c |g\rangle, \quad (18)$$

where $\hat{S}_{(m)}^+(t-t_m) = \sum_{j=1}^N \beta_j^{(m)}(\Delta_j, t-t_m) \hat{S}_+^j$ describes a collective single atomic excitation caused by the absorption of the m -th photonic qubit at the time $t \approx t_m$. All M atomic excitations are decoupled from each other for $M \ll N$ and in the case of strong reciprocal dephasing. Such separable quantum state of M qubits in QRAM can be formally written as a product $|Q_{RAM}\rangle = |g_c\rangle \prod_{m=1}^M |D_m\rangle$, where M states are orthogonal $\langle D_{m'} | D_m \rangle \sim \delta_{m,m'}$. The state $|D_m\rangle$ can be interpreted as the state of m -th QM cell where t_m is a time-label of this cell (rephasing/dephasing of the atomic coherence in this cell).

In the case when the m' -th atomic excitation will irradiate the stored photon qubit, when the initial quantum

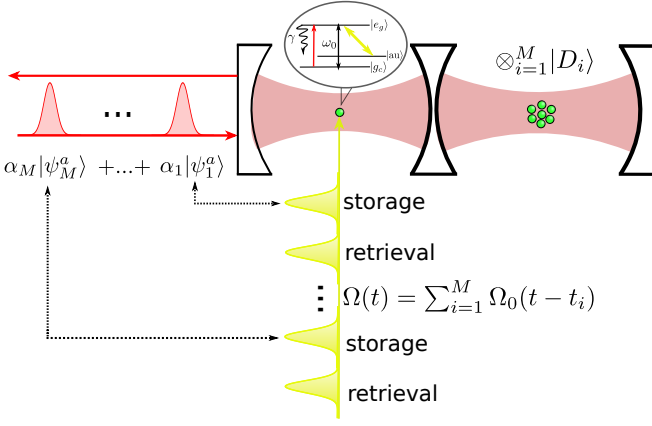


FIG. 4. (Color online) Quantum addressing is implemented by the synchronization between the readout from the QM unit and the quantum control of three-level atom. The quantum information is retrieved from QM as the sequence of M time-bin single photon. During the readout of each photon the control atom is transferred into the superposition of states $|g\rangle_c$ and $|a_u\rangle_c$ via lambda-transition by the classical control field $\Omega(t)$ and the single photon ($\sum_j^M |\Psi_j^a\rangle$) distributed in M time-bins (quantum address). Retrieval pulses return the atom to the ground state before each new addressing wave packet.

state of QRAM and light is transformed as follows:

$$\begin{aligned}
 &|0\rangle_f |Q_{RAM}\rangle \rightarrow -|\psi_{in,m'}\rangle_f \hat{S}_{(M)}^+(t - t_M) \\
 &\quad \dots \hat{S}_{(m'+1)}^+(t - t_{m'+1}) \hat{S}_{(m'-1)}^+(t - t_{m'-1}) \\
 &\quad \dots \hat{S}_{(1)}^+(t - t_1) |g_c\rangle |g\rangle \\
 &\equiv -|\psi_{in,m'}\rangle_f |g_c\rangle |\emptyset_{m'}\rangle \prod_{m \neq m'}^M |D_m\rangle, \quad (19)
 \end{aligned}$$

where $M-1$ photon qubits are stored in the QM and m' -qubit has been irradiated in the quantum state $|\psi_{in,m'}\rangle_f$, $|\emptyset_{m'}\rangle$ means the empty m' cell of QM. Analogously, if m' -th and m'' -th stored qubits are irradiated from QRAM, the output state will be $|0\rangle_f |Q_{RAM}\rangle \rightarrow |\psi_{in,m'}\rangle_f |\psi_{in,m''}\rangle_f |g_c\rangle |\emptyset_{m'}\rangle |\emptyset_{m''}\rangle \prod_{m \neq m', m''}^M |D_m\rangle$ with two retrieved photon qubits etc.

For the addressing qubit we use a single photon wavepacket distributed in M time-bins (M coincides with the number of photon qubits stored in QM) that is described by the following quantum superposition $|\Psi^a\rangle_f = \sum_{n=1}^M \alpha_n |\psi_n^a(t)\rangle_f$ (where $|\psi_n^a(t)\rangle_f = |\psi^a[-(t - (n-1)\tau_o - t_c)]\rangle_f$ and the duration of each time-bin is much smaller than the distance between two nearest time-bins $\delta z/c \ll T_0$, $\sum_n |\alpha_n|^2 = 1$; $|\psi^a(t)\rangle_f = \int dz g(t - z/c, \delta z_f) e^{-i\omega(t-z/c)} \hat{a}^\dagger(z) |0\rangle_f$ which is stored within the independent temporal mode (where $\hat{a}^\dagger(z)$ is the Fourier transform of the creation operator in the momentum space $\hat{a}^\dagger(z) = \frac{1}{\sqrt{2\pi}} \int dk e^{-i(k-\omega_0/c)z} \hat{a}^\dagger(k)$; $[\hat{a}(z), \hat{a}^\dagger(z')] = \delta(z-z')$); $g(t)$ describes the temporal shape of the photon

wave packet; δz is its spatial longitudinal size). At the time $t \approx t_c$ we map the first wave packet on the control atom state $|a_u\rangle$ via Raman transition as it is sketched in Fig. 4. These M photon wave packets provide the orthogonality for all M quantum addresses. Such single photon state can be prepared by using the photon echo QM [23] or by the stimulated rapid adiabatic passage that was successfully implemented with the high efficiency [24].

By taking into account the initial state $|\Psi_{in}\rangle = |\Psi^a\rangle_f |Q_{RAM}\rangle$, we consider how the addressing protocol works for the readout process. At first we analyze the retrieval stage for the 1-st addressing wave packet ($n = 1: 1 \leq n \leq M$) of $|\Psi^a\rangle_f$. The first wave packet and the control laser pulse provide all together the Raman resonant transfer of the control atom $|g_c\rangle \rightarrow |a_u\rangle$ that leads to the following state

$$\begin{aligned}
 &|\Psi_{in}\rangle \rightarrow |\Psi_1\rangle \\
 &= |0\rangle_{out,f} \prod_{m=1}^M |D_m\rangle \left(|g_c\rangle \sum_{n=2}^M \alpha_n |\psi_n^a\rangle_f \right. \\
 &\quad \left. - \alpha_1 |a_u\rangle |0\rangle_f \right), \quad (20)
 \end{aligned}$$

where $|0\rangle_{out,f}$ denotes the vacuum state of the output light field modes. Herein, the field mode of the second QED cavity is shifted out from the resonance with the field mode of the first QED cavity during the interaction with the control atom that can be implemented by using the acoustic-optical modulator in the second QED cavity. In particular, the highly efficient mapping (20) of the photon wave packet on the control atom state $|a_u\rangle$ is possible for the exponentially rising shape $g(-t)$ [25]. The exponential shape $g(t)$ corresponds to the typical photon irradiation by the single two-level system. At the same time $g(-t)$ can be put into practice via various generalized time-reversal CRIB schemes [26].

In the next step we retrieve the first photon qubit from QM by rephasing the atomic coherence in the QM ensemble. Here, we return the atomic ensemble in resonance with the two QED cavity modes and rephase only the 1-st atomic coherence of the state $|\phi_1(t)\rangle$ during the readout process by inverting the frequency detuning of each atom $\Delta_j \rightarrow -\Delta_j$. The atomic rephasing will lead to the transfer of the 1-st atomic state $|D_1\rangle$ into the free propagating photon wave packet or returns to the atomic ensemble in the case of the atomic blockade. These two alternatives of the qRAM operation happen in accordance with the analyzed two basic regimes (1-st or 2-nd) determined by two control atom states ($|g_c\rangle$ or $|a_u\rangle$). Eventually these two quantum alternatives lead to the following transformation of the state $|\Psi_1\rangle$:

$$\begin{aligned}
|\Psi_1\rangle \rightarrow |\Psi_2\rangle &= |0\rangle_{out,f} \prod_{m=2}^M |D_{in,m}\rangle \\
&\{ \alpha_1 |au_c\rangle |\emptyset_1\rangle |\psi_{in,1}\rangle_f \\
&+ |g_c\rangle |\phi_{in,1}\rangle \sum_{n=2}^M \alpha_n |\psi_n^a\rangle_f \}. \quad (21)
\end{aligned}$$

Next we return the excited state $|au_c\rangle$ of the control atom to the initial state $|g_c\rangle$ by the retrieval of the first time-bin photon wave packet via applying an additional laser pulse on the transition $|au_c\rangle \rightarrow |e_c\rangle$ (see Fig. 4). This atomic transfer $|e_c\rangle$ leads to the following transition

$$\begin{aligned}
|\Psi_2\rangle &\rightarrow |\Psi_3\rangle \\
&= \prod_{m=2}^M |\phi_{in,m}\rangle \{ -\alpha_1 |g_c\rangle |\emptyset_1\rangle |\psi_1^a\rangle_f |\psi_{in,1}\rangle_f \\
&+ |g_c\rangle |\phi_{in,1}\rangle |0\rangle_{out,f} \sum_{n=2}^M \alpha_n |\psi_n^a\rangle_f \}. \quad (22)
\end{aligned}$$

The light field component of the state (22) is characterized by the two entangled photon wave packets irradiated by the control atom and by the atomic ensemble of qRAM at two different moments of time. We repeat this process one by one for the second and all others $M - 1$ time-bin addressing wave packets that leads to the following output state:

$$\begin{aligned}
|\Psi_{in}\rangle &\rightarrow |\Psi_{out}\rangle = \\
&= \sum_n^M \alpha_n |g_c\rangle |\emptyset_n\rangle |\psi_n^a\rangle_f |\psi_{in,n}\rangle_f \prod_{m \neq n}^M |D_m\rangle \quad (23)
\end{aligned}$$

As it is seen in Eq.(23), the two photon field is irradiated in the entangled state of the addressed and retrieved photons. The final state is a result of the pure unitary evolution leading to the quantum superposition of M two-photon states - $|\psi_n^a\rangle_f, |\psi_{in,n}\rangle_f$ with amplitudes determined by the addressing states that accomplishes the qRAM operation on the multi-qubit QM. We note that other $(M - 1)$ -stored qubits $|\phi_{in,m}\rangle$ become also entangled with the two photon qubits that is done through the superposition of the states $|\psi_n^a\rangle_f |\psi_{in,n}\rangle_f |\phi_{in,1}\rangle, \dots, |\phi_{in,n-1}\rangle, |\phi_{in,n+1}\rangle, |\phi_{in,M}\rangle$. It is obvious, that the performed analysis is valid for the arbitrary initial quantum state of the QM atomic ensemble, for example, entangled with another freedom degrees of its environment. Finally, we note that by exploiting the time-reverse symmetry of the light-atom interaction we can implement the quantum addressing

storage of the photonic qubit. Thus we showed the possibility of the effective implementation of the multi-qubit qRAM based on the photon echo QM and three-level atom incorporated in two coupled QED-cavities.

EXPERIMENTAL ISSUES

Nowadays it seems promising to implement the proposed qRAM in the circuit and nano-optical QED schemes. All basic required hardware elements are implemented in the circuit QED: system of two coupled cavities with quantum emitters [27], the multi-qubit echo memory of the spin ensemble coupled to the cavity is under the active development [18] as well as the coherent transfer of the single artificial atom population [28–30]. The technique of the multi-time-bin photon generation, which was successfully demonstrated in the cavity QED [24], can also be applied to microwave domain [28, 31]. For the optical domain there are several potential candidates: quantum dots (QD) in coupled photonic crystal nano-cavities [32], nanofibers coupled to cavities with solid-state emitters (like NV centers in diamond, QD, rare-earth ions doped crystals) [33] or natural atoms [34, 35]. Open optical cavities [36] can also be used.

However, it is worth noting that the qRAM operation requires the further improvement of the control atom integration in the QED cavity. Various developing protocols of photon routing [37] can be applied for the effective photon addressing. The passive routing [35, 38], which does not require any control fields, seems especially promising.

CONCLUSION

We proposed the scheme of qRAM based on the single multi-qubit QM. The qRAM contains two coupled QED cavities with the control three-level atom and the resonant atomic ensemble. The multimodality is achieved by combining the time-domain control of the single three-level atom in the cavity together with the photon echo multimode QM. The multi-time-bin photon state establish the addressing by setting the control atom in the superposition of transfer and blockade regimes. We found a series of impedance matching conditions for the physical parameters of the scheme providing the broadband efficient implementation of qRAM processes. The performed analysis can be easily extended to various variants of the photon echo QM protocols in the impedance matching QED cavities that essentially enlarges the potential for the experimental implementation. The proposed qRAM can be realized with current technologies of the circuit and cavity QED that seems promising for using in superconducting quantum computing and optical quantum communications. Unlike the bucket-brigade architecture

[5, 6], the proposed qRAM avoids the complex control on many optically coupled QM cells since it can be implemented in a single compact device containing multi-qubit quantum memory cell that seems promising for practice. Finally, we note that the proposed qRAM can be developed for off-resonant Raman atomic transitions that will provide the direct quantum storage on the long-lived atomic transition and facilitate the experimental implementation of the qRAM impedance matching conditions.

ACKNOWLEDGMENTS

The authors are grateful to A. V. Akimov, E. Giacobino, A. Lvovsky and L. Maccone for useful and stimulating discussions. We thank the Russian Scientific Fund through the grant no. 14-12-01333 for financial support of this work.

* samoi@yandex.ru

- [1] V. Giovannetti, S. Lloyd, and L. Maccone, Phys. Rev. Lett. **100**, 230502 (2008).
- [2] G. Brassard, P. Høyer, and A. Tapp, SIGACT News **28**, 14 (1997).
- [3] A. Ambainis, SIAM Journal on Computing **37**, 210 (2007), <http://dx.doi.org/10.1137/S0097539705447311>.
- [4] P. J. Clarke, R. J. Collins, V. Dunjko, E. Andersson, J. Jeffers, and G. S. Buller, Nature communications **3**, 1174 (2012).
- [5] V. Giovannetti, S. Lloyd, and L. Maccone, Phys. Rev. Lett. **100**, 160501 (2008); Phys. Rev. A **78**, 052310 (2008).
- [6] F.-Y. Hong, Y. Xiang, Z.-Y. Zhu, L.-z. Jiang, and L.-n. Wu, Phys. Rev. A **86**, 010306 (2012).
- [7] H. Kimble, Nature **453**, 1023 (2008).
- [8] Z.-L. Xiang, S. Ashhab, J. Q. You, and F. Nori, Rev. Mod. Phys. **85**, 623 (2013).
- [9] S. A. Moiseev and S. Kröll, Phys. Rev. Lett. **87**, 173601 (2001).
- [10] W. Tittel, M. Afzelius, T. Chanelière, R. Cone, S. Kröll, S. Moiseev, and M. Sellars, Laser & Photonics Reviews **4**, 244 (2010).
- [11] M. P. Hedges, J. J. Longdell, Y. Li, and M. J. Sellars, Nature **465**, 1052 (2010).
- [12] M. Hosseini, B. M. Sparkes, G. Campbell, P. K. Lam, and B. C. Buchler, Nat Commun **2**, 174 (2011); M. Hosseini, G. Campbell, B. M. Sparkes, P. K. Lam, and B. C. Buchler, Nature Physics **7**, 794 (2011); B. M. Sparkes, J. Bernu, M. Hosseini, J. Geng, Q. Glorieux, P. Altin, P. K. Lam, N. P. Robins, and B. C. Buchler, New Journal of Physics **15**, 085027 (2013).
- [13] D. Rieländer, K. Kutluer, P. M. Ledingham, M. Gündoğan, J. Fekete, M. Mazzer, and H. de Riedmatten, Phys. Rev. Lett. **112**, 040504 (2014).
- [14] N. Sinclair, E. Saglamyurek, H. Mallahzadeh, J. A. Slater, M. George, R. Ricken, M. P. Hedges, D. Oblak, C. Simon, W. Sohler, and W. Tittel, Phys. Rev. Lett. **113**, 053603 (2014).
- [15] V. Damon, M. Bonarota, A. Louchet-Chauvet, T. Chanelière, and J.-L. L. Gouët, New Journal of Physics **13**, 093031 (2011).
- [16] M. Afzelius and C. Simon, Phys. Rev. A **82**, 022310 (2010); S. A. Moiseev, S. N. Andrianov, and F. F. Gubaidullin, Phys. Rev. A **82**, 022311 (2010).
- [17] M. Sabooni, Q. Li, S. Kröll, and L. Rippe, Phys. Rev. Lett. **110**, 133604 (2013).
- [18] B. Julsgaard, C. Grezes, P. Bertet, and K. Mølmer, Phys. Rev. Lett. **110**, 250503 (2013); M. Afzelius, N. Sangouard, G. Johansson, M. U. Staudt, and C. M. Wilson, New Journal of Physics **15**, 065008 (2013); K. I. Gerasimov, S. A. Moiseev, V. I. Morosov, and R. B. Zaripov, Phys. Rev. A **90**, 042306 (2014); C. Grezes, B. Julsgaard, Y. Kubo, M. Stern, T. Umeda, J. Isoya, H. Sumiya, H. Abe, S. Onoda, T. Ohshima, V. Jacques, J. Esteve, D. Vion, D. Esteve, K. Mølmer, and P. Bertet, Phys. Rev. X **4**, 021049 (2014).
- [19] S. A. Moiseev and S. N. Andrianov, Journal of Physics B: Atomic, Molecular and Optical Physics **45**, 124017 (2012).
- [20] S. A. Moiseev, Bull. Russ. Acad. Sci. Phys **68** (2004); B. Kraus, W. Tittel, N. Gisin, M. Nilsson, S. Kröll, and J. I. Cirac, Phys. Rev. A **73**, 020302 (2006); T. Chanelière, Opt. Express **22**, 4423 (2014).
- [21] D. F. Walls and G. J. Milburn, *Quantum optics* (Springer, 2007).
- [22] S. A. Moiseev, Phys. Rev. A **88**, 012304 (2013).
- [23] S. A. Moiseev and B. S. Ham, Phys. Rev. A **70**, 063809 (2004).
- [24] P. B. R. Nisbet-Jones, J. Dille, A. Holleczek, O. Barter, and A. Kuhn, New Journal of Physics **15**, 053007 (2013).
- [25] A. V. Gorshkov, A. André, M. Fleischhauer, A. S. Sørensen, and M. D. Lukin, Phys. Rev. Lett. **98**, 123601 (2007).
- [26] E. S. Moiseev and S. A. Moiseev, New Journal of Physics **15**, 105005 (2013); G. T. Campbell, O. Pinel, M. Hosseini, T. C. Ralph, B. C. Buchler, and P. K. Lam, Phys. Rev. Lett. **113**, 063601 (2014).
- [27] J. Raftery, D. Sadri, S. Schmidt, H. E. Türeci, and A. A. Houck, Phys. Rev. X **4**, 031043 (2014).
- [28] B. Johnson, M. Reed, A. Houck, D. Schuster, L. S. Bishop, E. Ginossar, J. Gambetta, L. DiCarlo, L. Frunzio, S. Girvin, *et al.*, Nature Physics **6**, 663 (2010).
- [29] A. A. Abdumalikov, O. Astafiev, A. M. Zagoskin, Y. A. Pashkin, Y. Nakamura, and J. S. Tsai, Phys. Rev. Lett. **104**, 193601 (2010).
- [30] M. A. Sillanpää, J. Li, K. Cicak, F. Altomare, J. I. Park, R. W. Simmonds, G. S. Paraoanu, and P. J. Hakonen, Phys. Rev. Lett. **103**, 193601 (2009).
- [31] M. Pechal, L. Huthmacher, C. Eichler, S. Zeytinoglu, A. A. Abdumalikov, S. Berger, A. Wallraff, and S. Filipp, Phys. Rev. X **4**, 041010 (2014).
- [32] S. Hughes, Phys. Rev. Lett. **98**, 083603 (2007).
- [33] R. Yalla, M. Sadgrove, K. P. Nayak, and K. Hakuta, Phys. Rev. Lett. **113**, 143601 (2014).
- [34] J. D. Thompson, T. G. Tiecke, N. P. de Leon, J. Feist, A. V. Akimov, M. Gullans, A. S. Zibrov, V. Vuletić, and M. D. Lukin, Science **340**, 1202 (2013).
- [35] I. Shomroni, S. Rosenblum, Y. Lovsky, O. Bechler, G. Guendelman, and B. Dayan, Science **345**, 903 (2014).
- [36] P. Jobez, I. Usmani, N. Timoney, C. Laplane, N. Gisin, and M. Afzelius, New Journal of Physics **16**, 083005 (2014).

- [37] S. Rosenblum, S. Parkins, and B. Dayan, Phys. Rev. A **84**, 033854 (2011).
 [38] K. Koshino, S. Ishizaka, and Y. Nakamura, Phys. Rev. A **82**, 010301 (2010); J. Gea-Banacloche and L. M. Pe-drotti, Phys. Rev. A **86**, 052311 (2012).

Supplementary materials

Hamiltonian and basic equations

The Hamiltonian of the analyzed system is $\hat{H} = \hat{H}_0 + \hat{H}_1$, where

$$\begin{aligned} \hat{H}_0 = & \hbar\omega_0 \left(\sum_{j=1}^N S_z^j + S_z^0 + a_1^\dagger a_1 + a_2^\dagger a_2 \right. \\ & \left. + \int d\omega \left(\sum_m \hat{c}_m^\dagger(\omega) \hat{c}_m(\omega) + b^\dagger(\omega) b(\omega) \right) \right), \end{aligned} \quad (\text{A.24})$$

is the basic Hamiltonian, and the perturbation part is

$$\begin{aligned} \hat{H}_1 = & \hbar \sum_{j=1}^N \Delta_j \hat{S}_z^j + \hbar \delta S_z^0 \\ & + \hbar \int d\nu \nu \hat{b}^\dagger(\omega_0 + \nu) \hat{b}(\omega_0 + \nu) \\ & + \hbar \sum_m \int d\nu \nu \hat{c}_m^\dagger(\omega_0 + \nu) \hat{c}_m(\omega_0 + \nu) + \\ & + \hbar f_1 \int d\nu (\hat{a}_1^\dagger \hat{b}(\omega_0 + \nu) + H.C.) \\ & + \hbar \left(g_1 \hat{a}_1^\dagger \hat{S}_-^0 + f_2 \hat{a}_1^\dagger \hat{a}_2 + g_2 \sum_{j=1}^N \hat{a}_2^\dagger \hat{S}_-^j + H.C. \right) \\ & + \hbar \sqrt{\frac{\gamma}{2\pi}} \sum_m \int d\nu \left(\hat{c}_m(\omega_0 + \nu) \hat{S}_+^0 + H.C. \right), \end{aligned} \quad (\text{A.25})$$

where the first three terms are determined by frequency detunings of the j -th atom Δ_j in QM, δ of the control atom and the detuning ν of the free field modes; four further terms are the interactions between the second cavity mode and atoms (with the coupling constant g_2), between free field modes and the first cavity mode (with the coupling constant f_1), and the interaction between the cavity mode and the control atom (with the coupling constant g_1), and the interaction between the coupled cavity modes (with the coupling constant f_2); \hat{S}_z^0 , \hat{S}_z^j are the z projection of the spin 1/2 operators, \hat{S}_+^j , \hat{S}_-^j and \hat{S}_+^0 , \hat{S}_-^0 are the transition spin operators of j -th and control atoms; $\hat{a}_{1,2}^\dagger$ and $\hat{a}_{1,2}$ are arising and decreasing operators of the 1-st and 2-nd cavity field modes; $b^\dagger(\omega)$, $b(\omega)$ are the bozonic operators of free propagating modes ($[b(\omega), b^\dagger(\omega')] = \delta(\omega - \omega')$).

By assuming that the QED cavity modes and all the atoms and bath modes $c_m(\omega)$ are in the ground state, the initial wave function in the case of the input single photon field $|\Psi(t \rightarrow -\infty)\rangle = \int d\omega \alpha_\omega^0 b^\dagger(\omega) |0\rangle$ and total wavefunction is given by Eq.(1). By using the well-known input-output formalism we obtain the following system of equations

$$\frac{d\alpha_1}{dt} = -ig_1\beta_c - if_2\alpha_2 - \frac{\kappa}{2}\alpha_1 + \sqrt{\kappa}\alpha_{in}(t), \quad (\text{A.26})$$

$$\frac{d\beta_c}{dt} = -i(\delta - i\gamma/2)\beta_c - ig_1\alpha_1, \quad (\text{A.27})$$

$$\frac{d\alpha_2}{dt} = -ig_2 \sum_{j=1}^N \beta_j - if_2\alpha_1, \quad (\text{A.28})$$

$$\frac{d\beta_j}{dt} = -i(\Delta_j - i/T_2)\beta_j - ig_2\alpha_2, \quad (\text{A.29})$$

where $\kappa = 2\pi f_1^2$, also we have phenomenologically added the weak decay constant $1/T_2$ for the atomic coherence QM caused by the interaction with local fluctuating fields

$$\sqrt{\kappa}\alpha_{in}(t) = -if_1 \int d\nu \alpha_\nu^o e^{-i\nu t}. \quad (\text{A.30})$$

Integrating equation (A.27)

$$\begin{aligned} \beta_j(\tau) &= -ig_2 \int_{-\infty}^{\tau} dt' \alpha_2(t') e^{-i(\Delta_j - i/T_2)(\tau - t')} \Big|_{\lim_{\tau \gg \delta t}} \\ &\cong -i2\pi g_2 \tilde{\alpha}_2(\Delta_j) e^{-i(\Delta_j - i/T_2)\tau}, \end{aligned} \quad (\text{A.31})$$

where pulse duration of the light field δt is assumed to be short enough in comparison with the atomic decoherence time of the atomic QM $\delta t \ll T_2$. Inserting it into Eq.(A.28) and using the Fourier transform $\alpha_{1,2,in}(t) = \int d\nu \tilde{\alpha}_{1,2,in}(\nu) \exp\{-i\nu t\}$, and $\beta_c(t) = \int d\nu \tilde{\beta}_c(\nu) \exp\{-i\nu t\}$ we find the following solution for the amplitudes of the control atom and two cavity modes:

$$\tilde{\beta}_c = g_1 \frac{\tilde{\alpha}_1}{(\nu - \delta + i\gamma/2)}, \quad (\text{A.32})$$

$$\tilde{\alpha}_2(\nu) = A_{2,1}(\nu) \tilde{\alpha}_1(\nu), \quad (\text{A.33})$$

$$\tilde{\alpha}_1(\nu) = A_{1,in}(\nu) \tilde{\alpha}_{in}(\nu), \quad (\text{A.34})$$

where

$$A_{1,in}(\nu) = \frac{i\sqrt{\kappa}}{\nu + i\kappa/2 - \frac{g_1^2}{(\nu - \delta + i\gamma/2)} - \frac{f_2^2}{\nu + iNg_2^2\tilde{G}(\nu)}}, \quad (\text{A.35})$$

$$A_{2,1}(\nu) = \frac{f_2}{\nu + iNg_2^2\tilde{G}(\nu)}. \quad (\text{A.36})$$

Readout stage

The system of equations is almost the same as (A.26, A.27, A.28,A.29), however, we take into account the absence of the driving field, inverted inhomogeneous broadening at the reference time $t = \tau$:

$$\frac{d\alpha_1}{dt} = -ig_1\beta_1 - if_2\alpha_2 - \frac{\kappa}{2}\alpha_1, \quad (\text{A.37})$$

$$\frac{d\beta_c}{dt} = -i(\delta - i\gamma/2)\beta_c - ig_1\alpha_1, \quad (\text{A.38})$$

$$\frac{d\alpha_2}{dt} = -ig_2 \sum_{j=1}^N \beta_j - if_2\alpha_1, \quad (\text{A.39})$$

$$\frac{d\beta_j}{dt} = i(\Delta_j + i/T_2)\beta_j - ig_2\alpha_2. \quad (\text{A.40})$$

By taking into account the initial condition at $t = \tau$ in accordance with Eq.(2)

$$\beta_j(-\Delta_j, \tau) = i\sqrt{2\pi\kappa}\frac{g_2}{f_2}F_S(\Delta_j)\alpha_{\Delta_j}^0 e^{-i(\Delta_j - i/T_2)\tau}, \quad (\text{A.41})$$

and $\alpha_1 = \alpha_2 = \beta_c = 0$, after the storage stage. By solving the linear system of equations (A.36)-(A.39), we find the following spectral component of the irradiated single photon field

$$\begin{aligned} \alpha_\nu(t) &= i\sqrt{2\pi\kappa}\frac{g_2}{f_2}F_R(\nu)\beta(\nu, \tau) \cdot \\ &G_L(\nu) \exp\{-i\nu(t - \tau) - \tau/T_2\}, \end{aligned} \quad (\text{A.42})$$

where $F_R(\nu)$ indicates the spectral transfer function for the readout stage.

Blockade: wave function of atomic system

For the blockade regime we find the following Fourier image for the amplitude of the QM atomic excitation in the calculations Eqs.(A.36-A.39) for the retrieval stage:

$$\begin{aligned} \beta_B(\Delta, \nu) &= \frac{1}{1/T_2 - i\nu - i\Delta} \cdot \\ &\left(\beta(\Delta, 0) + \Delta_{in}J(\nu)(F_B(\nu) - 1) \int d\Delta' \frac{G(\Delta')\beta(\Delta', 0)}{-i\nu + i\Delta'} \right), \end{aligned} \quad (\text{A.43})$$

where the index "B" means the blockade regime and

$$J(\nu) = \frac{\kappa(\kappa - 2i\nu)}{\kappa^2 - 4i\kappa\nu - 8\nu^2}. \quad (\text{A.44})$$

In the case of the strong atomic blockade $2 + 4C \gg 1$:

$$\begin{aligned} \beta_B(\Delta, \nu) &\cong \frac{1}{1/T_2 - i\nu - i\Delta} \cdot \\ &\left(\beta_0(\Delta, 0)e^{-i\Delta\tau} - \frac{2\Delta_{in}^2 J(\nu)}{(\nu^2 + \Delta_{in}^2)}\beta_0(-\nu, 0)e^{i\nu\tau - \tau/T_2} \right), \end{aligned} \quad (\text{A.45})$$

where $\beta_0(-\nu, 0) = i\sqrt{2\pi\kappa}\frac{g_2}{f_2}F(-\nu)\alpha_{-\nu}^0 e^{-\tau/T_2}$. By taking into account $J(\nu \approx 0) \approx 1$ and $\tau \ll T_2$, we obtain quite perfect recovery of the atomic amplitude for $|\nu| < \kappa$:

$$\beta_B(\Delta, |\nu| < \kappa) |_{\tau \ll T_2} = -\frac{1}{1/T_2 - i\nu - i\Delta}\beta(\Delta, 0). \quad (\text{A.46})$$

As it is seen in Eq.(A45), atomic dynamics during the irradiation and subsequent reabsorption of the echo pulse leads to the additional π -phase shift of the atomic coherence for $t \gg t_{echo} = 2\tau$.